Electronic Supplementary Information

Amino Acid Modified Copper Electrodes for the Enhanced Selective Electroreduction of Carbon Dioxide towards Hydrocarbons

Ming Shi Xie,[a] Bao Yu Xia,[a] Yawei Li,[b] Ya Yan,[a] Yanhui Yang,[a] Qiang Sun,[b] Siew Hwa Chan,[c] Adrian Fisher,[d] and Xin Wang[a]*

[a] M. S. Xie, Dr. B. Y. Xia, Y. Yan, Prof Y. H. Yang, Prof. X. Wang

School of Chemical and Biomedical Engineering, Nanyang Technological University,

62 Nanyang Drive, Singapore 637459, Singapore

[b] Y. W. Li , Prof. Q. Sun

Singapore-Peking University Research Centre, Campus for Research Excellence & Technological Enterprise (CREATE), Singapore 138602, Singapore

Department of Materials Science and Engineering, Peking University, Beijing 100871, China

[c] Prof. S. H. Chan

School of Mechanical & Aerospace Engineering, Nanyang Technological University,

50 Nanyang Avenue, Singapore 639798, Singapore

[d] Prof. A. Fisher

Department of Chemical Engineering and Biotechnology, University of Cambridge, New Museums Site, Pembroke Street, Cambridge, CB2 3RA, UK

‡ Mr. M. S. Xie, Dr. B. Y. Xia and Mr. Y. W. Li contributed equally to this work.

Correspondence and requests for materials should be addressed to Prof X. Wang: E-mail: WangXin@ntu.edu.sg

Experimental details:

Materials. Potassium persulfate (≥99.0%), phosphoric acid (≥85 wt. %), potassium bicarbonate (99.7%), 1-aminoanthraquinone (97%), sodium nitrite (97%), Acetonitrile (99%), and tetrabutylammonium tetrafluoroborate (99%) were purchased from Sigma-Aldrich. Glycine (≥99%), DL-alanine (≥99%), DL-leucine (≥99%), DL-tryptophan (≥99%), stearic acid (≥98.5) were purchased from Sigma. Copper foil (0.025mm thick, 99.98%), DL-tyrosine (99%), DL-arginine (≥98%), 1-dodecyl mercaptan (≥98%) and o-nitroaniline (98%) were purchased from Aldrich. Sodium hydroxide (97%) was purchased from Alfa Aesar. Hydrochloric acid (37%) was purchased from Merck. Carbon dioxide gas (99.8%) was purchased from Air Liquide. Chemicals were all used without purification. Chemical bath and electrolyte solution were prepared with deionized water, which is produced by Milli-Q Gradient A10 system (Millipore).

Thickness calculation. The thickness of the film is estimated to be 0.8 μm via the equation: thickness=Q*M/nFρ (Q: charge for reducing $Cu(OH)_2$ film per cm^2, in our test is ~0.55C; $M(Cu(OH)_2)$=97.5g mol^{-1}; n=2; ρ=3.37 g cm^{-3}; F= 96485 C mol^{-1}).

Electrochemical active surface measurements. The electrochemically active surface area of electrodes was measured through determination of double-layer capacitance at various scan rates. CVs were obtained for a potential range in which only double-layer adsorption and desorption occurred. The current densities were obtained by integrating area of CV curves, and then plotted against the scan rates of the CV. The slope of the linear regression gave the capacitance. Cu NW film electrodes in 0.05 M H_2SO_4 provided a capacitance of 1.25 mF cm^{-2}. As a comparison, polished Cu foils gave out a capacitance of 1.15×10^{-2} mF cm^{-2}.

Current densities measurements. A Cu disk electrode (diameter 2.0 mm) was polished with 0.01 μm aluminum and washed with deionized water under ultrasonic condition. Cu disk electrodes were immersed

into 1.0 mM and 0.01 mM glycine solution for various duration (1 min or 15 mins) to prepare modified ones. Modified Cu disk electrodes and bare Cu disk electrodes were used for scanning between -0.4 V and -1.9 V vs. Ag/AgCl (scan rate: 0.1 V s^{-1}) in 0.1 M $KHCO_3$ solution, before test the electrolyte was bubbled by with N_2 for 1 h.

Table S1. Faradaic Efficiencies of CO_2 electro-reduction products under different conditions.

Electrode (vs. Ag/AgCl)	Faradaic efficiency (%)						
	CH_4	C_2H_4	C_2H_6	C_3H_6	CO	H_2	Total
Cu NW film Gly (-1.9 V)	N/A	12.7	21.1	0.3	0.9	52.2	87.2
Cu NW film Gly (-1.8 V)	N/A	8.3	18.0	0.3	1.0	69.3	97.0
Cu NW film Gly (-1.7 V)	N/A	5.1	12.4	0.3	1.0	76.5	95.2
Cu NW film Gly (-1.6 V)	N/A	3.5	8.4	0.3	1.1	77.4	90.7
Cu NW film Gly (-1.5 V)	N/A	2.1	5.0	0.2	1.6	79.3	88.2
Cu NW film Gly (-1.4 V)	N/A	1.3	3.3	0.2	2.0	85.4	92.3
Cu NW film Gly (-1.3 V)	N/A	0.8	2.6	0.2	3.3	84.8	91.8
Cu NW film (-1.9 V)	N/A	5.9	11.7	0.2	0.7	76.2	94.7
Cu NW film (-1.8 V)	N/A	5.3	11.1	0.2	0.8	75.9	93.3
Cu NW film (-1.7 V)	N/A	4.0	9.9	0.3	0.8	78.6	93.5
Cu NW film (-1.6 V)	N/A	3.0	6.7	0.2	0.8	82.8	93.5
Cu NW film (-1.5 V)	N/A	2.3	4.5	0.2	1.1	80.0	88.0
Cu NW film (-1.4 V)	N/A	1.4	2.8	0.2	1.6	90.5	96.5
Cu NW film (-1.3 V)	N/A	0.7	1.6	0.2	2.5	89.1	94.1
Cu NW film Leu (-1.9 V)	N/A	6.1	13.0	0.2	0.6	72.4	92.4
Cu NW film Trp (-1.9 V)	N/A	8.8	18.0	0.3	0.7	67.3	95.2
Cu NW film Arg (-1.9 V)	N/A	8.3	15.1	0.2	0.7	63.2	87.5
Cu NW film Ala (-1.9 V)	N/A	8.8	15.3	0.2	0.7	66.8	91.8
Cu NW film Tyr (-1.9 V)	N/A	8.8	11.8	0.3	0.7	72.3	93.9
Cu NW film Gly after 2 h (-1.9 V)	N/A	13.8	20.0	0.3	0.5	63.2	97.8
Cu NW film Gly after 3 h (-1.9 V)	N/A	12.8	18.7	0.3	0.5	66.8	98.6
Cu NW film Gly after 4 h (-1.9 V)	N/A	13.0	19.1	0.4	1.0	65.2	98.7
Cu NW film Gly after 5 h (-1.9 V)	N/A	12.7	17.3	0.7	0.3	64.3	95.3
Cu NW film Gly after 12 h (-1.9 V)	N/A	9.0	13.4	0.2	3.2	70.9	96.7
Cu NW film Gly 4×10^{-6} m mol (-1.9 V)	N/A	8.0	13.7	0.2	0.7	74.3	96.8
Cu NW film Gly 2×10^{-6} m mol (-1.9 V)	N/A	7.1	16.8	0.2	0.7	69.7	94.4
Cu NW film Gly 1×10^{-4} m mol (-1.9 V)	N/A	5.3	15.0	0.1	0.5	71.5	92.5
Cu NW film Gly 4×10^{-4} m mol (-1.9 V)	N/A	4.9	9.3	0.1	0.5	79.3	94.2
Cu NW film RCOOH (-1.9 V)	N/A	3.7	12.1	0.1	0.5	79.6	96.0

Cu NW film $PhNO_2$ (-1.9 V)	N/A	2.4	7.3	0.2	0.8	77.1	87.8
Cu NW film AQ (-1.9 V)	N/A	1.9	6.7	0.2	0.7	83.1	92.6
Cu NW film RSH (-1.9 V)	N/A	2.8	10.2	0.1	0.8	74.3	88.2
Cu foil (-1.9 V)	16.1	9.5	N/A	N/A	1.1	66.8	93.5
Cu foil (-1.8 V)	8.8	8.2	N/A	N/A	1.2	77.9	96.1
Cu foil (-1.7 V)	2.6	3.3	N/A	N/A	1.9	84.8	92.6
Cu foil (-1.6 V)	1.6	1.9	N/A	N/A	2.0	90.7	96.2
Cu foil (-1.5 V)	0.9	0.6	N/A	N/A	14.9	71.4	87.8
Cu foil Gly (-1.9 V)	32.1	24.0	N/A	N/A	0.6	34.7	91.5
Cu foil Gly (-1.8 V)	20.9	22.4	N/A	N/A	1.0	43.9	88.1
Cu foil Gly (-1.7 V)	12.2	18.0	N/A	N/A	4.1	56.5	90.9
Cu foil Gly (-1.6 V)	6.6	11.3	N/A	N/A	6.9	71.3	96.1
Cu foil Gly (-1.5 V)	4.3	6.9	N/A	N/A	5.8	71.3	88.3
Cu foil Leu (-1.9 V)	16.5	9.0	N/A	N/A	1.0	65.2	91.6
Cu foil Leu (-1.8 V)	12.0	10.2	N/A	N/A	1.7	65.8	89.6
Cu foil Leu (-1.7 V)	6.0	6.6	N/A	N/A	2.5	73.4	88.5
Cu foil Leu (-1.6 V)	3.0	3.6	N/A	N/A	4.8	81.8	93.2
Cu foil Leu (-1.5 V)	1.9	2.0	N/A	N/A	7.9	76.6	88.4
Cu foil Tyr (-1.9 V)	21.3	13.9	N/A	N/A	0.8	57.0	93.1
Cu foil Tyr (-1.8 V)	12.8	12.8	N/A	N/A	1.1	60.5	87.2
Cu foil Tyr (-1.7 V)	9.7	12.4	N/A	N/A	1.7	67.6	91.4
Cu foil Tyr (-1.6 V)	5.7	9.1	N/A	N/A	2.5	75.0	92.3
Cu foil Tyr (-1.5 V)	3.6	6.0	N/A	N/A	3.2	76.3	89.1
Cu foil Arg (-1.9 V)	24.3	15.9	N/A	N/A	1.0	47.1	88.4
Cu foil Arg (-1.8 V)	21.7	17.3	N/A	N/A	0.8	55.1	94.9
Cu foil Arg (-1.7 V)	14.2	15.0	N/A	N/A	3.5	56.8	89.5
Cu foil Arg (-1.6 V)	9.4	9.8	N/A	N/A	4.3	71.5	95.1
Cu foil Arg (-1.5 V)	4.8	5.1	N/A	N/A	3.6	74.1	87.6
Cu foil Ala (-1.9 V)	25.5	18.4	N/A	N/A	2.9	41.6	88.4
Cu foil Ala (-1.8 V)	19.5	18.3	N/A	N/A	1.0	56.4	95.1
Cu foil Ala (-1.7 V)	14.5	15.2	N/A	N/A	2.5	63.1	95.2
Cu foil Ala (-1.6 V)	7.5	9.5	N/A	N/A	6.6	70.9	94.4
Cu foil Ala (-1.5 V)	4.9	5.7	N/A	N/A	5.9	79.4	96.0
Cu foil Trp (-1.9 V)	28.6	11.1	N/A	N/A	1.3	48.0	89.0
Cu foil Trp (-1.8 V)	29.3	11.8	N/A	N/A	2.4	46.7	90.3
Cu foil Trp (-1.7 V)	19.1	11.5	N/A	N/A	4.2	60.2	95.0
Cu foil Trp (-1.6 V)	6.0	5.7	N/A	N/A	4.4	79.0	95.2
Cu foil Trp (-1.5 V)	5.2	4.6	N/A	N/A	6.1	71.2	87.0
Cu foil Gly 5×10^{-6} m mol (-1.9	7.1	16.8	N/A	N/A	1.1	63.7	88.7

V)							
Cu foil Gly 5×10^{-8} m mol (-1.9 V)	27.3	17.6	N/A	N/A	1.1	46.4	92.4
Cu foil RCOOH (-1.9 V)	12.4	10.4	N/A	N/A	3.9	65.6	92.3
Cu foil $PhNO_2$ (-1.9 V)	7.3	5.2	N/A	N/A	1.9	80.6	94.9
Cu foil AQ (-1.9 V)	7.7	5.1	N/A	N/A	3.5	74.6	90.9
Cu foil RSH (-1.9 V)	13.2	9.0	N/A	N/A	1.8	71.0	95.1
Annealed Cu Gly (-1.9 V)	5.3	19.7	0.3	N/A	1.1	61.2	87.6
Annealed Cu Gly (-1.8 V)	4.5	21.3	0.4	N/A	1.1	66.5	93.9
Annealed Cu Gly (-1.7 V)	2.8	18.6	0.4	N/A	1.4	65.0	88.2
Annealed Cu Gly (-1.6 V)	1.8	14.6	0.5	N/A	2.8	71.2	90.9
Annealed Cu Gly (-1.5 V)	1.7	11.9	0.6	N/A	2.9	78.1	95.3
Annealed Cu Gly (-1.4 V)	1.1	7.4	0.6	N/A	3.9	78.4	91.5
Annealed Cu Gly (-1.3 V)	1.3	5.6	0.8	N/A	7.5	79.7	94.8
Annealed Cu (-1.9 V)	0.6	7.0	0.5	N/A	1.2	86.8	96.0
Annealed Cu (-1.8 V)	0.6	8.9	0.7	N/A	1.1	84.3	95.7
Annealed Cu (-1.7 V)	0.4	8.8	1.0	N/A	2.1	78.6	91.0
Annealed Cu (-1.6 V)	0.4	7.5	1.1	N/A	3.0	80.0	92.1
Annealed Cu (-1.5 V)	0.4	6.0	1.3	N/A	3.4	79.0	90.1
Annealed Cu (-1.4 V)	0.5	4.5	1.3	N/A	6.6	82.2	95.1
Annealed Cu (-1.3 V)	0.8	3.8	1.4	N/A	12.9	71.1	90.0
Annealed Cu Arg (-1.9 V)	5.9	12.6	0.2	N/A	1.0	76.9	96.6
Annealed Cu Leu (-1.9 V)	1.3	9.4	0.5	N/A	1.2	79.2	91.5
Annealed Cu Tyr (-1.9 V)	2.3	10.8	0.5	N/A	1.2	75.8	90.6
Annealed Cu Trp (-1.9 V)	1.5	18.7	1.1	N/A	1.3	67.5	90.0
Annealed Cu Ala (-1.9 V)	2.8	18.1	0.7	N/A	1.3	67.3	90.3

Table S2. FEs of hydrocarbon products on various kinds of Cu electrodes.

Electrodes	Potential (V, vs. Ag/AgCl)	Faraday efficiency (%)				Reference
		CH_4	C_2H_4	C_2H_6	C_3H_6	
Cu foil+Gly	-1.9	32	24	N/A	N/A	This work
Cu NW+Gly	-1.9	N/A	6.7	13	0.16	
Annealed Cu+Gly	-1.9	5.3	20	0.4	N/A	
Cu foil	-2.1	20	4	N/A	N/A	*Electrochimica Acta*, **2001**, *46*, 3015–3022
Cu nanofoam	-1.7	0.2	1.4	1.2	0.1	*ACS Catal*, **2014**, *4*, 3091−3095
Reduction Cu_2O film	-1.6	N/A	4	7	N/A	*J Am Chem Soc*, **2012**, *134*, 7231−7234
Carbon-supported Cu	-1.8	18	38	N/A	N/A	*ACS Catal*, **2014**, *4*, 3682−3695
copper electrodeposits	-1.9	N/A	10	3	N/A	*Electrochimica Acta*, **2013**, *102*, 388– 392
Cu2O-derived copper nanoparticles	-1.75	3	19	2	N/A	*Phys Chem Chem Phys*, **2014**, *16*, 12194-12201
Nanoparticles covered Cu	-1.75	2	36	N/A	N/A	*Phys Chem Che. Phys*, **2012**, *14*, 76–81
Sputtered Cu	-1.75	7	22	1	N/A	*Phys Chem Chem Phys*, **2012**, *14*, 76–81
Cu nanoparticles 5-15 nm	-1.75	15	7	N/A	N/A	*J Am Chem Soc*, **2014**, *136*, 6978−6986
Cu overlayers on Pt	-1.65	7	N/A	N/A	N/A	*J Phys Chem C*, **2013**, *117*, 20500−20508
Cu(111) single crystals	-1.9	24	3	N/A	N/A	*Electrocatal*, **2012**, *3*, 139–146

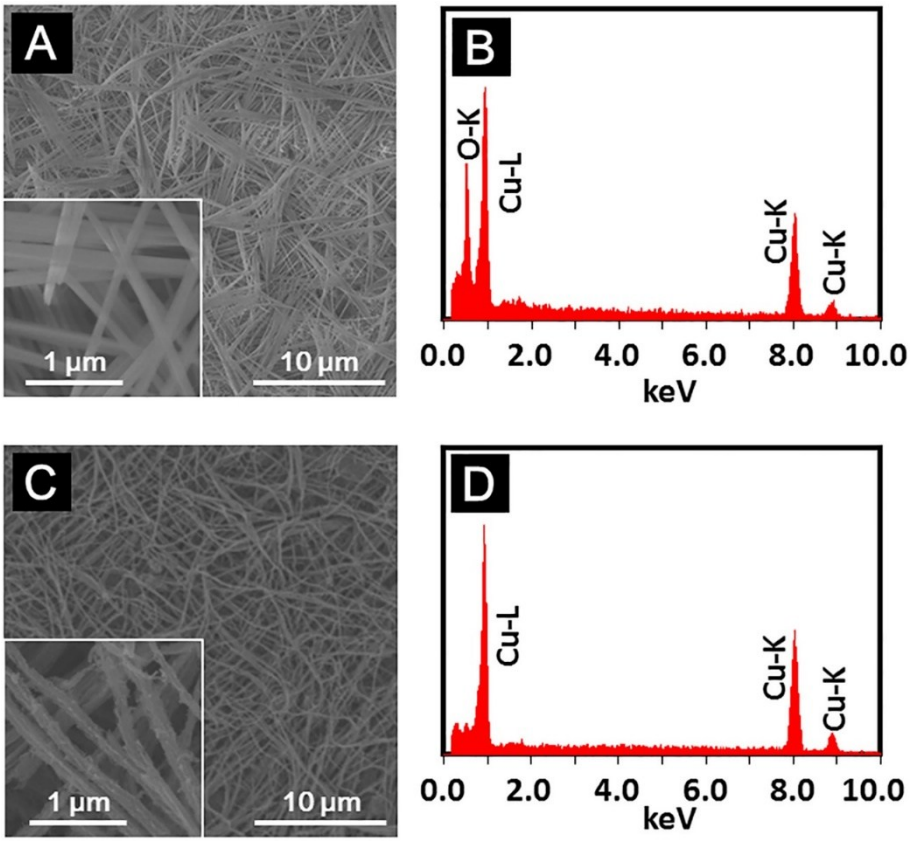

Figure S1. FESEM images and EDX patterns of $Cu(OH)_2$ (A, B) and Cu NW film (C, D).

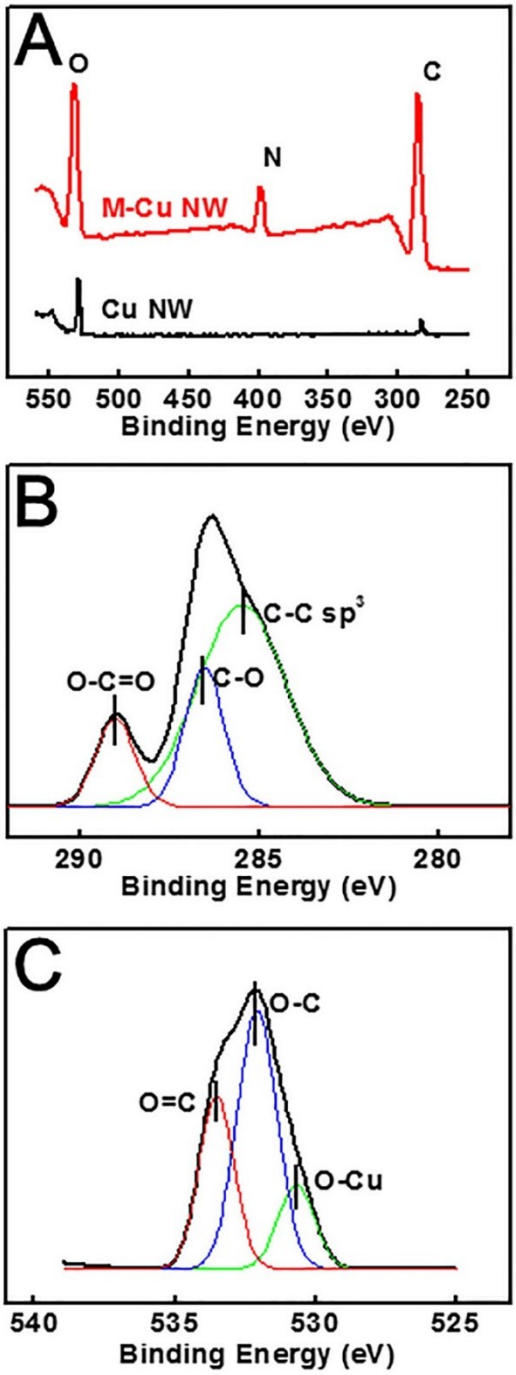

Figure S2. XPS patterns of Cu NW film and modified Cu NW film (pre-electrolysis). (A) Comparison on full range, (B) C1s scan and (C) O1s scan.

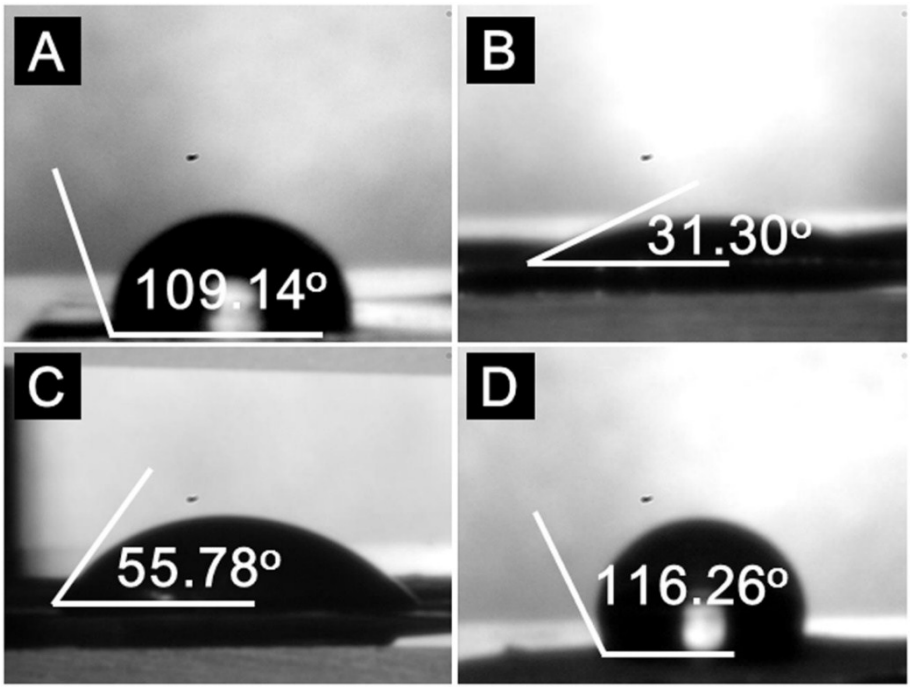

Figure S3. Contact angles of Cu foil (A), Cu NW film (B), 20μL 1mM glycine modified Cu NW film (C), large amount of glycine modified Cu NW film (D).

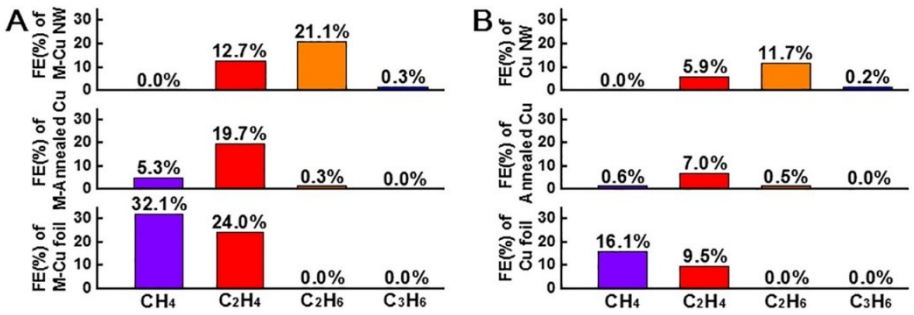

Figure S4. (A) Faradic efficiencies of hydrocarbons for different bare Cu (A) and modified Cu (B) electrodes.

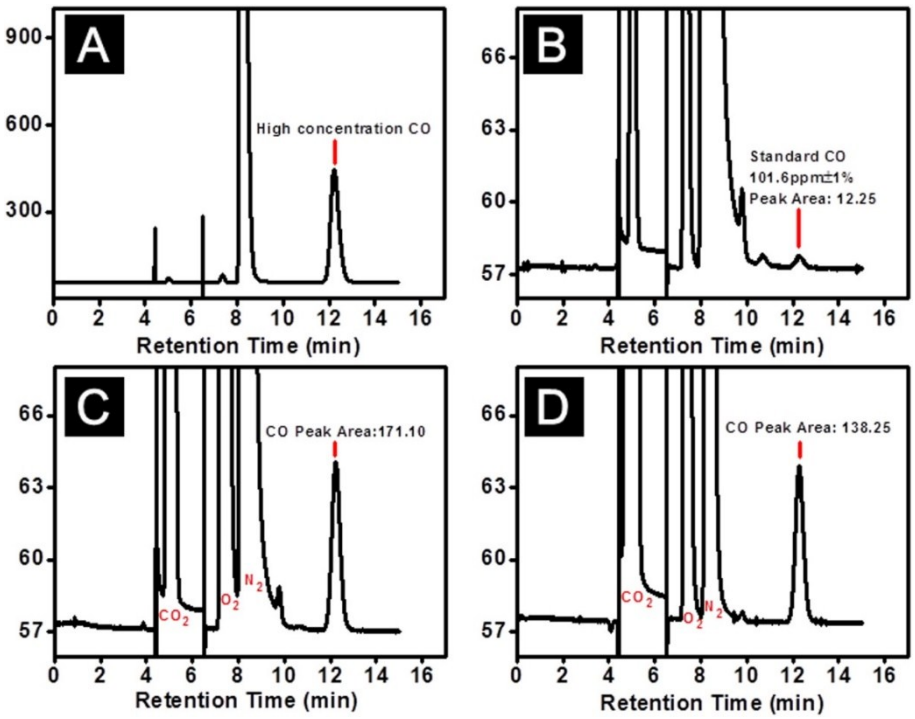

Figure S5. GC measurements of CO. (A) High concentration of CO, around 10%. (B) Standard sample of HCOOH, with a concentration of 101.6ppm±1%. (C) Sample of modified Cu NW Film. (D) Sample of Cu NW Film.

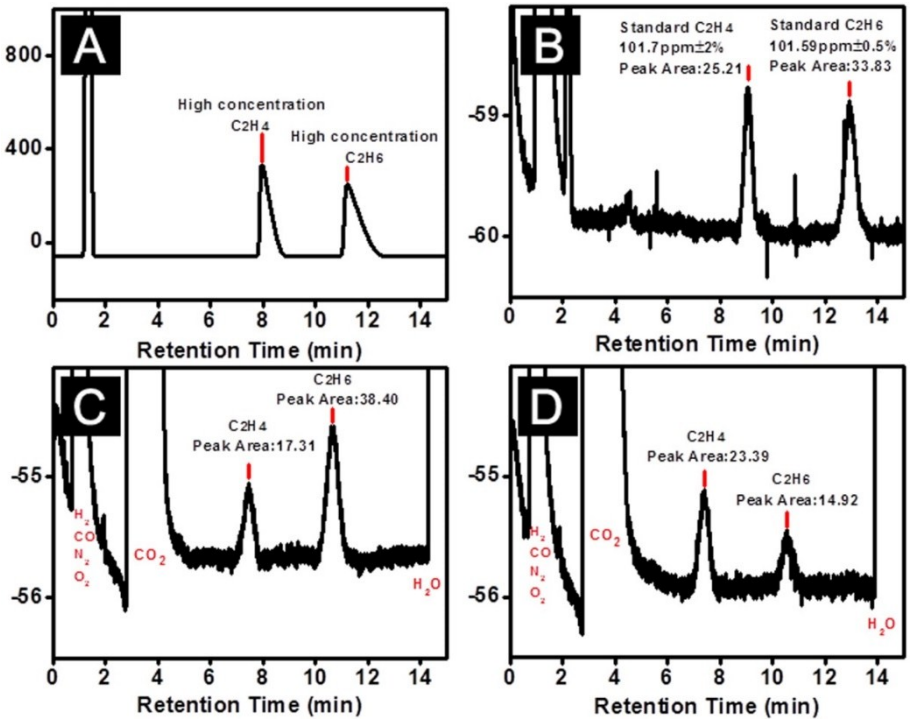

Figure S6. GC measurements of C_2H_4 and C_2H_6. (A) High concentration of C_2H_4 and C_2H_6, all around 5%. (B) Standard sample of C_2H_4 and C_2H_6, with a concentration of 101.7ppm±2%, 101.59ppm±0.5%, respectively. (C) Sample of modified Cu NW Film. (D) Sample of Cu NW Film.

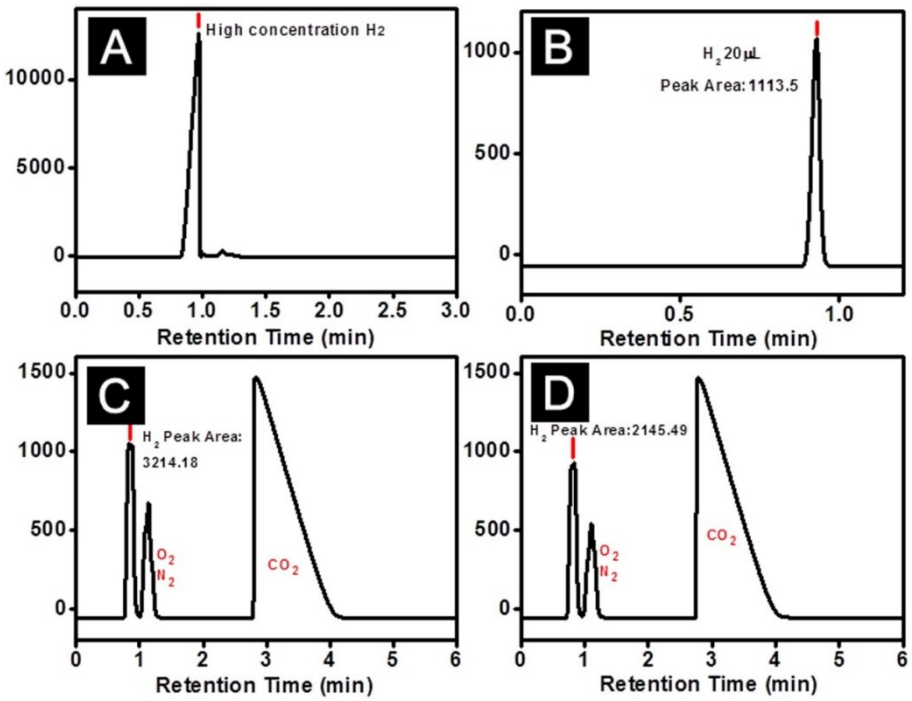

Figure S7. GC measurements of H_2. (A) High concentration of H_2 almost 100%. (B) Standard sample of H_2, with a concentration of 4000ppm. (C) Sample of modified Cu NW Film. (D) Sample of Cu NW Film.

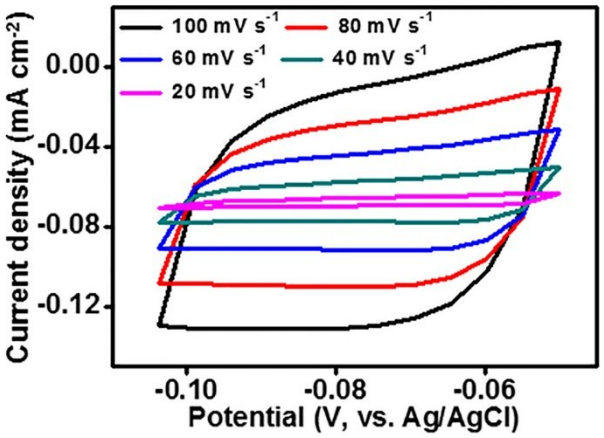

Figure S8. CVs of Cu NW film electrodes at various scan rates with double-layer charging and discharging, in a solution of 0.05 M H_2SO_4 solution.

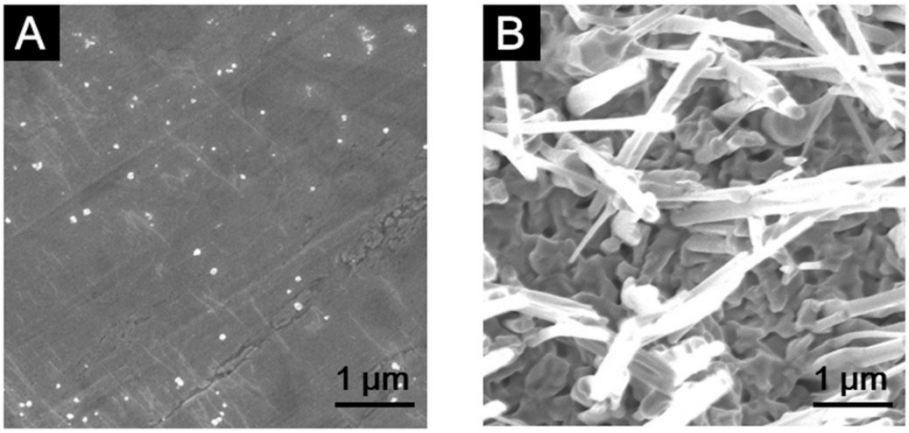

Figure S9. FESEM images of polished Cu foil (A) and annealed Cu (B).

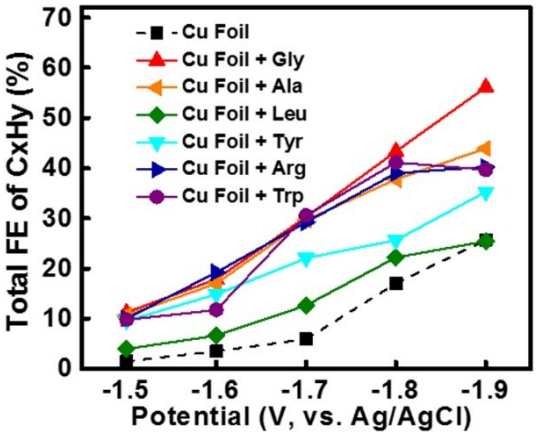

Figure S10. Total FEs of hydrocarbons on Cu foil electrodes modified with various amino acids in full potential range.

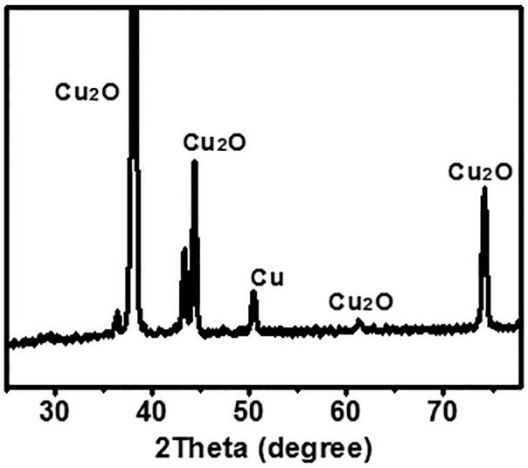

Figure S11. XRD pattern of annealed Cu (Cu_2O layer).

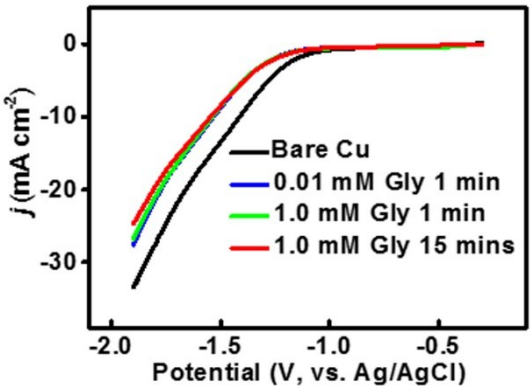

Figure S12. Linear sweep voltammograms for the bare and modified Cu disk electrodes (2.0 mm in diameter) in N_2 bubbled 0.1 $KHCO_3$ solution. Range: -0.4 V~ -1.9 V vs. Ag/AgCl. Scan rate: 0.1 V s^{-1}.

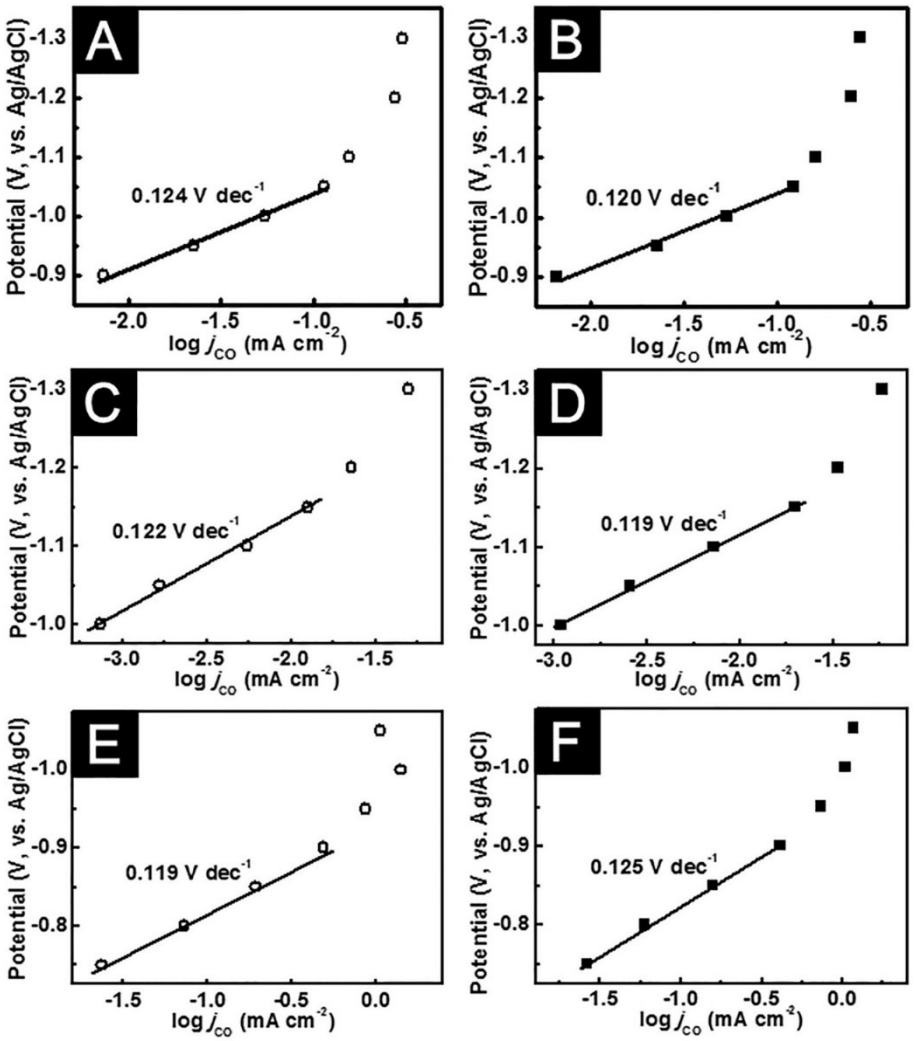

Figure S13. CO partial current density Tafel plots for Cu NW film electrode(A) and modified Cu NW film electrode(B) CO partial current density Tafel plots for Cu foil electrode (C), modified Cu foil electrode (D), annealed Cu electrode (E) and modified annealed Cu electrode (F).

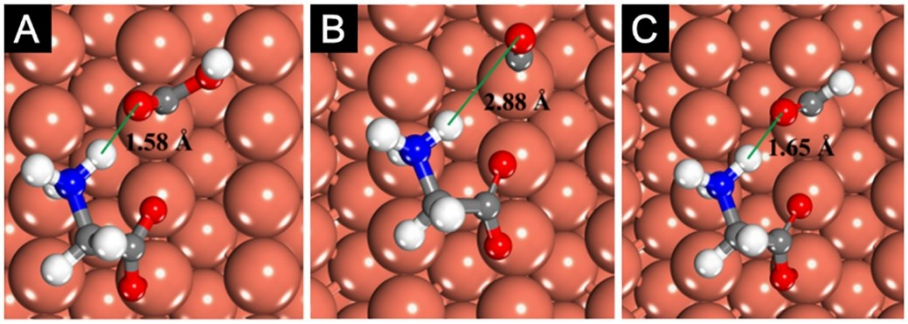

Figure S14. Hydrogen-bond like interaction between adsorbed amino acid and: (A) COOH*; (B) CO*; (C) CHO*.

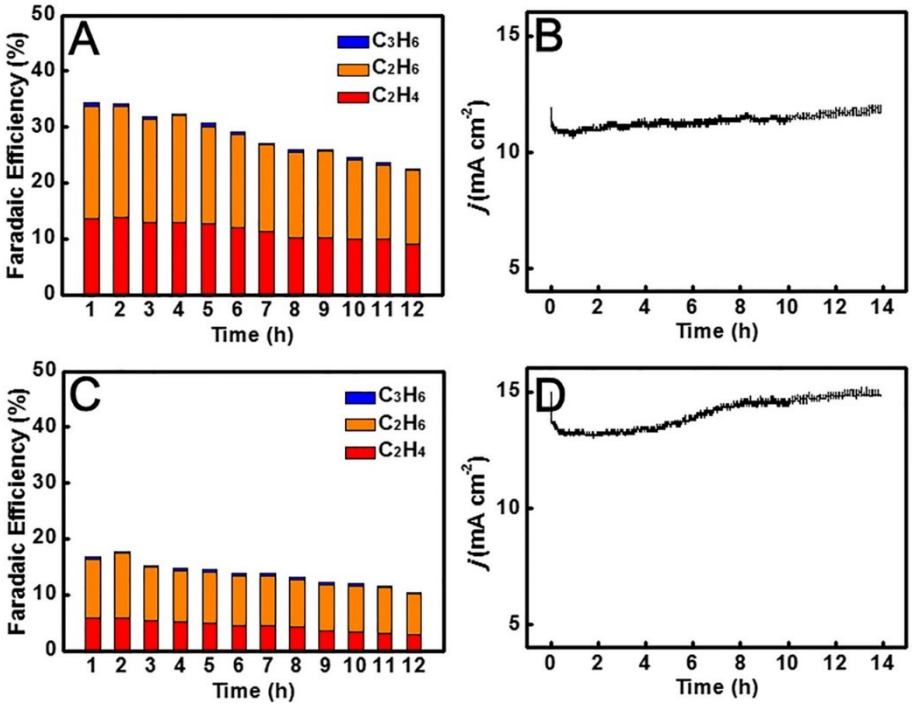

Figure S15. Electrocatalytic stability of modified Cu NW film (A, B) and bare Cu NW film (C, D) in CO_2 saturated $KHCO_3$ solution at -1.9 V: (A, C) Faradaic efficiencies; (B, D) the response of current density.

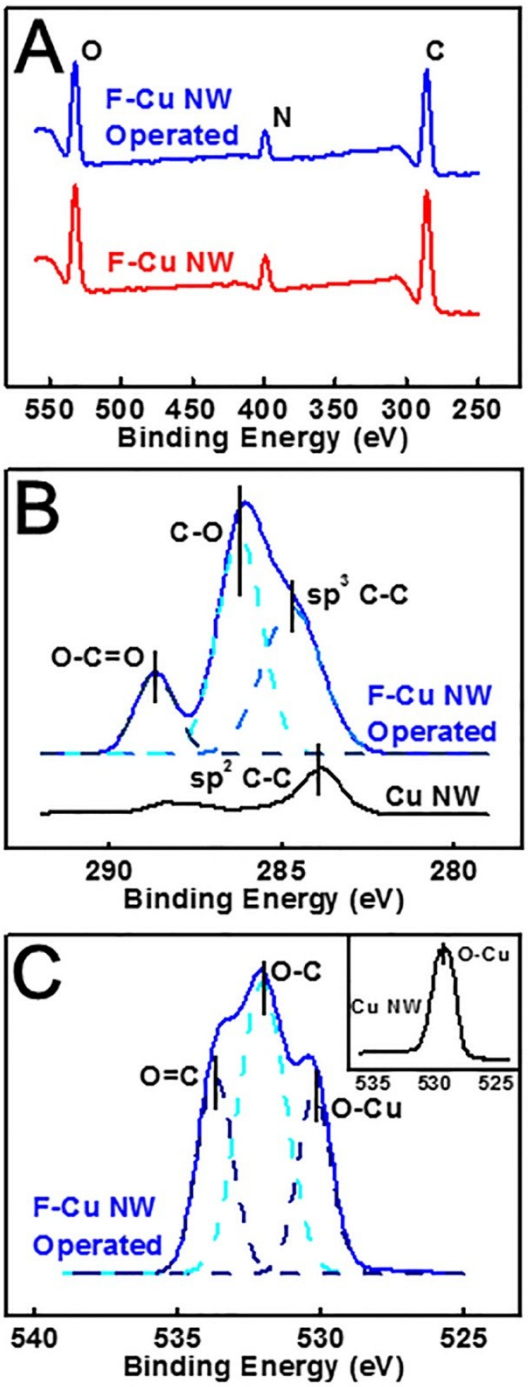

Figure S16. XPS patterns of the modified Cu NW film, after long time electrolysis at -1.9 V. (A) Comparison in full range, (B) C1s scan and (D) O1s scan.

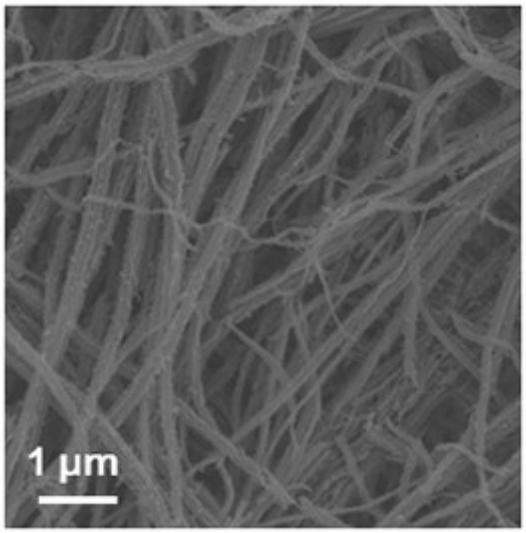

Figure S17. (A) FESEM image of the modified Cu NW film surface after long time electrolysis at -1.8 V.